2010 IEEE International Symposium on
Electromagnetic Compatibility

Multi-Physics Analysis Methodologies for Signal Integrity

Lijun Jiang

EEE, the University of Hong Kong (Associate Professor)
IBM EDA, IBM T. J. Watson Research Center (LOA)

ljiang@eee.hku.hk

OUTLINES

- **Multi-physics vs. Frequencies**
  - Helmholtz Decomposition
  - Evanescent Waves and Propagating Waves
  - Algorithm Dependencies
- **Multi-physics Thermal Electrical Coupling Analysis**
  - Thermal Conduction Modeling
  - Novel Equivalent Thermal Conductivity Calculation
  - Thermal Guideline Study
  - Thermal-electrical Coupling Simulation
- **Conclusions**

MAXWELL'S EQUATIONS

And GOD said

	Differential Form	Integral Form
Gauss's Law	$\nabla \cdot \mathbf{D} = \rho_f$	$\oint\!\!\!\oint_{\partial V} \mathbf{D} \cdot \mathrm{d}\mathbf{A} = Q_f(V)$
Gauss's Law for Magnetism	$\nabla \cdot \mathbf{B} = 0$	$\oint\!\!\!\oint_{\partial V} \mathbf{B} \cdot \mathrm{d}\mathbf{A} = 0$
Faraday's Law	$\nabla \times \mathbf{E} = -\frac{\partial \mathbf{B}}{\partial t}$	$\oint_{\partial S} \mathbf{E} \cdot \mathrm{d}\mathbf{l} = -\frac{\partial \Phi_{B,S}}{\partial t}$
Ampere's Law	$\nabla \times \mathbf{H} = \mathbf{J}_f + \frac{\partial \mathbf{D}}{\partial t}$	$\oint_{\partial S} \mathbf{H} \cdot \mathrm{d}\mathbf{l} = I_{f,S} + \frac{\partial \Phi_{D,S}}{\partial t}$
Continuity Equation	$\nabla \cdot \mathbf{J} = -\frac{\partial \rho}{\partial t}$	$\oint_{\partial S} \mathbf{J} \cdot ds = -\frac{\partial Q}{\partial t}$

and THEN there was light.

MAXWELL'S EQUATIONS

$$\nabla \times \mathbf{E} = -\frac{\partial \mathbf{B}}{\partial t}$$

$$\nabla \times \mathbf{H} = \mathbf{J}_f + \frac{\partial \mathbf{D}}{\partial t}$$

$$\nabla \cdot \mathbf{J} = -\frac{\partial \rho}{\partial t}$$

Consider the coupling

$$\nabla \cdot \mathbf{D} = \rho_f$$

$$\nabla \cdot \mathbf{B} = 0$$

$$\nabla \times \mathrm{E} = 0$$

$$\nabla \times \mathrm{H} = \mathrm{J_f}$$

$$\nabla \cdot \mathrm{J} = -\frac{\partial \rho}{\partial t}$$

Consider no coupling

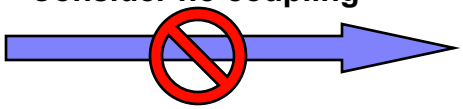

$$\nabla \cdot \mathbf{D} = \rho_f$$

$$\nabla \cdot \mathbf{B} = 0$$

HELMHOLTZ DECOMPOSITION

Let **F be a vector field on $\mathbf{R}^3$**, which is twice continuously differentiable and which vanishes faster than 1/*r* at infinity.[1] Then **F is a sum of a** gradient and a curl as follows:

$$\mathbf{F} = -\nabla\left(\mathcal{G}(\nabla \cdot \mathbf{F})\right) + \nabla \times \left(\mathcal{G}(\nabla \times \mathbf{F})\right)$$

where $\mathcal{G}$ represents the Newtonian potential operator. (When acting on a vector field, such as $\nabla \times \mathbf{F}$, **it is defined to act on each component.)**

If **F has zero** divergence, $\nabla \cdot \mathbf{F} = 0$, **then F is called solenoidal or divergence-free, and the Helmholtz decomposition of F collapses to**

$$\mathbf{F} = \nabla \times \mathcal{G}(\nabla \times \mathbf{F}) = \nabla \times \mathbf{A}.$$

In this case, **A is known as a** vector potential for **F. This particular choice of vector potential is divergence-free, which in physics is referred to as the** Coulomb gauge condition.

Likewise, if **F has zero** curl, $\nabla \times \mathbf{F} = 0$, **then F is called irrotational or curl-free, and the Helmholtz decomposition of F collapses to**

$$\mathbf{F} = -\nabla\,\mathcal{G}(\nabla \cdot \mathbf{F}) = -\nabla\varphi.$$

In this case, φ is known as a *scalar potential* for **F.**

In general **F is the sum of these two terms,**

$$\mathbf{F} = -\nabla\varphi + \nabla \times \mathbf{A}$$

where the negative gradient of the scalar potential is the irrotational component, and the curl of the vector potential is the solenoidal component.

Cited from: http://en.wikipedia.org/wiki/Helmholtz_decomposition

HELMHOLTZ DECOMPOSITION

- **Electric Field Integral Equation (EFIE) at Low Frequencies:**

$$-\mathbf{E}^i(\mathbf{r}) = i\omega\mu \int_S g(\mathbf{r},\mathbf{r}')\mathbf{J}(\mathbf{r}')d\mathbf{r}' - \frac{1}{i\omega\varepsilon}\nabla\int_S g(\mathbf{r},\mathbf{r}')\nabla'\cdot\mathbf{J}(\mathbf{r}')d\mathbf{r}'$$

$$\mathbf{E}^V(\mathbf{r}) \qquad\qquad \mathbf{E}^S(\mathbf{r})$$

$$\frac{|\mathbf{E}^V|}{|\mathbf{E}^S|} \propto O(k^2R^2), \qquad kR \to 0.$$

- **Scalar Helmholtz system for Dirichlet problems:**

$$-\phi^i(\mathbf{r}) = \int_S g(\mathbf{r},\mathbf{r}')J(\mathbf{r}')d\mathbf{r}', \qquad g(\mathbf{r},\mathbf{r}') = \frac{e^{ik|\mathbf{r}-\mathbf{r}'|}}{4\pi|\mathbf{r}-\mathbf{r}'|}$$

LOOP STAR DECOMPOSITION

- Loop Basis: divergence free
- Star Basis: quasi-curl-free.
- Tree Basis: RWG basis with the basis along a cut removed. The cut prevents the rest of the RWG basis (tree basis) from forming any loop.

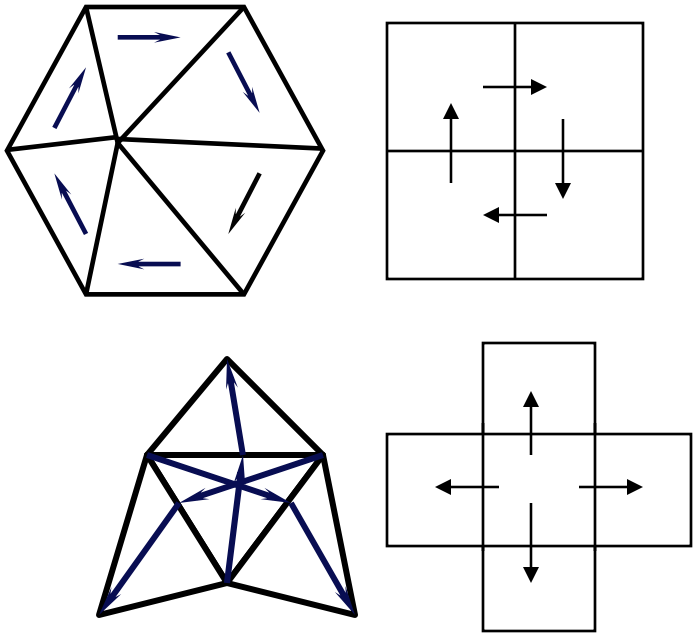

- LS or LT formulation isolates the contribution of vector potential and scalar potential.
- Information of vector potential will not be lost due to machine precision.

LOW FREQUENCY EFIE

- **EFIE with Loop-Tree Basis**
  - **The current density can be expanded as**

$$\mathbf{J}(r') = \mathbf{J}_L^t(\mathbf{r}') \cdot \mathbf{I}_L + \mathbf{J}_T^t(\mathbf{r}') \cdot \mathbf{I}_T$$

    - $\mathbf{J}_L$ **: Loop basis (divergence free)**
    - $\mathbf{J}_T$ **: Tree basis (non-divergence-free)**

$$\begin{bmatrix} \overline{\mathbf{Z}}_{LL} & \overline{\mathbf{Z}}_{LT} \\ \overline{\mathbf{Z}}_{TL} & \overline{\mathbf{Z}}_{TT} \end{bmatrix} \begin{bmatrix} \mathbf{I}_L \\ \mathbf{I}_T \end{bmatrix} = \begin{bmatrix} \mathbf{V}_L \\ \mathbf{V}_T \end{bmatrix}$$

  - **Impedance Matrix**

$$\overline{Z}_{LL} = i\omega\mu \left\langle \vec{J}_L(\vec{r}), g(\vec{r},\vec{r}'), \vec{J}_L^t(\vec{r}') \right\rangle$$

$$\overline{Z}_{LT} = i\omega\mu \left\langle \vec{J}_L(\vec{r}), g(\vec{r},\vec{r}'), \vec{J}_T^t(\vec{r}') \right\rangle = \overline{Z}_{TL}^t$$

$$\overline{Z}_{TT} = i\omega\mu \left\langle \vec{J}_T(\vec{r}), g(\vec{r},\vec{r}'), \vec{J}_T^t(\vec{r}') \right\rangle - \frac{i}{\omega\varepsilon} \left\langle \nabla \cdot \vec{J}_T(\vec{r}), g(\vec{r},\vec{r}'), \nabla' \cdot \vec{J}_T^t(\vec{r}') \right\rangle$$

FREQUENCY NORMALIZATION

- **Original matrix scaled in frequency**

$$\begin{bmatrix} \bar{\mathbf{Z}}_{LL}(O(\omega)) & \bar{\mathbf{Z}}_{LT}(O(\omega)) \\ \bar{\mathbf{Z}}_{TL}(O(\omega)) & \bar{\mathbf{Z}}_{TT}(O(\frac{1}{\omega})) \end{bmatrix} \begin{bmatrix} \mathbf{I}_L(O(1)) \\ \mathbf{I}_T(O(\omega)) \end{bmatrix} = \begin{bmatrix} \mathbf{V}_L(O(\omega)) \\ \mathbf{V}_T(O(1)) \end{bmatrix}$$

- **Normalized matrix scaled in frequency**

$$\begin{bmatrix} \frac{1}{\omega}\bar{\mathbf{Z}}_{LL}(O(1)) & \bar{\mathbf{Z}}_{LT}(O(\omega)) \\ \bar{\mathbf{Z}}_{TL}(O(\omega)) & \bar{\mathbf{Z}}_{TT}(O(1)) \end{bmatrix} \begin{bmatrix} \mathbf{I}_L(O(1)) \\ \frac{1}{\omega}\mathbf{I}_T(O(1)) \end{bmatrix} = \begin{bmatrix} \frac{1}{\omega}\mathbf{V}_L(O(1)) \\ \mathbf{V}_T(O(1)) \end{bmatrix}$$

- **Convergence is still slow**

$\bar{\mathbf{Z}}_{LL}$	**fast**

$\bar{\mathbf{Z}}_{CC}$	**slow**

FROM LF TO HF

At very low frequencies (loop-tree basis)

$$\begin{bmatrix} \frac{4}{i\omega\mu}\mathbf{Z}_{LL}(O(1)) & \frac{4}{\mu}\mathbf{Z}_{LC}\mathbf{K}^{-1}(O(\omega)) \\ \epsilon\mathbf{K}^{t-1}Z_{CL}(O(\omega)) & i\omega\epsilon\mathbf{K}^{t-1}(\mathbf{Z}_{CC}^{A}+\mathbf{Z}_{CC}^{V})\mathbf{K}^{-1}(O(1)) \end{bmatrix} \begin{bmatrix} \mathbf{I}_L(O(1)) \\ \mathbf{Q}(O(1)) \end{bmatrix} = \begin{bmatrix} \frac{4}{i\omega\mu}\mathbf{V}_L(O(1)) \\ \epsilon\mathbf{K}^{t-1}\mathbf{V}_C(O(1)) \end{bmatrix}$$

At mid frequencies (loop-tree basis)

$$\begin{bmatrix} \frac{4}{i\omega\mu}\mathbf{Z}_{LL}(O(1)) & \frac{4}{\mu}\mathbf{Z}_{LC}\mathbf{K}^{-1}(O(\omega)) \\ \epsilon\mathbf{K}^{t-1}Z_{CL}(O(\omega)) & i\omega\epsilon\mathbf{K}^{t-1}(\mathbf{Z}_{CC}^{A}+\mathbf{Z}_{CC}^{V})\mathbf{K}^{-1}(O(\omega^2)) \end{bmatrix} \begin{bmatrix} \mathbf{I}_L(O(1)) \\ \mathbf{Q}(O(1)) \end{bmatrix} = \begin{bmatrix} \frac{4}{i\omega\mu}\mathbf{V}_L(O(1)) \\ \epsilon\mathbf{K}^{t-1}\mathbf{V}_C(O(1)) \end{bmatrix}$$

At mid frequencies (RWG basis)

$$\left[i\omega\mu\langle\mathbf{\Lambda}_m, G, \mathbf{\Lambda}_n\rangle - \frac{i}{\omega\epsilon}\langle\nabla\cdot\mathbf{\Lambda}_m, G, \nabla\cdot\mathbf{\Lambda}_n\rangle\right][\mathbf{I}_n] = -\langle\mathbf{\Lambda}_m, \mathbf{E}^{inc}\rangle$$

- **Low frequency normalization based on the loop-tree basis is not valid for mid frequencies: loop-tree couplings become stronger and the impedance matrix becomes ill conditioned**
- **RWG based EFIE does not work well at very low frequencies**

Where is the boundary ?

FROM LF TO HF

0.0003GHz, $a = 0.001\lambda$

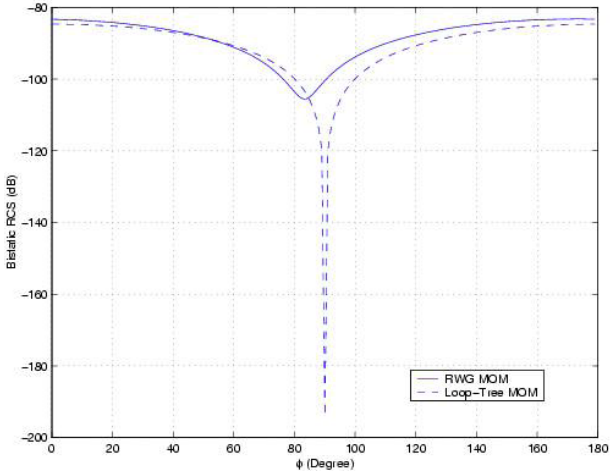

0.003GHz, $a = 0.01\lambda$

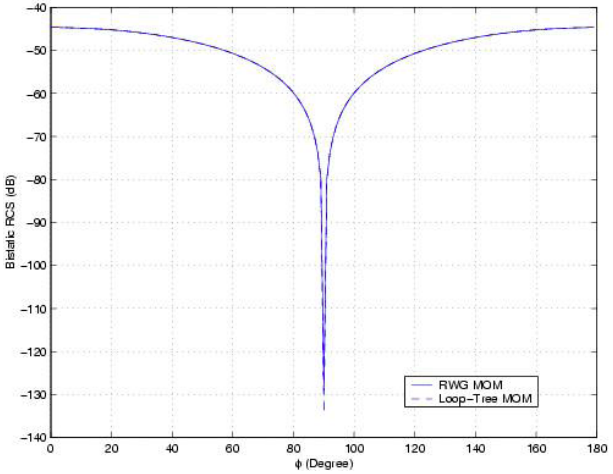

0.03GHz, $a = 0.1\lambda$

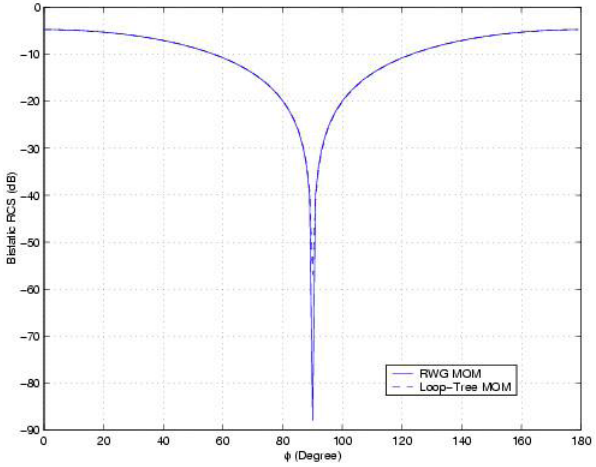

0.3GHz, $a = 1.0\lambda$

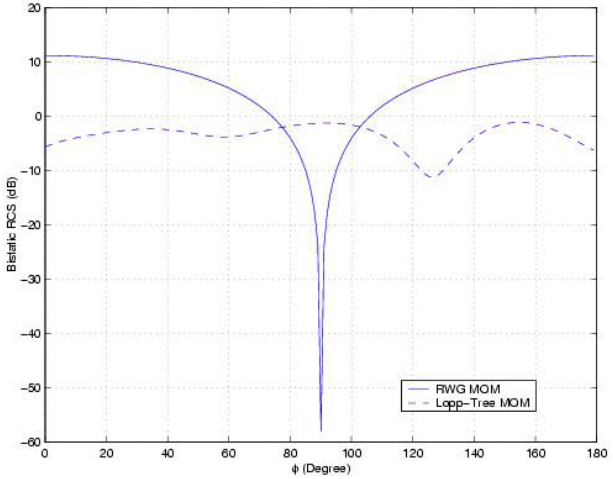

EVANESCENT AND PROPAGATING WAVES

- **Two different kernels**

Static Source.
e.g. charges

$$G = \frac{1}{r}$$

$$\frac{dG}{dr} = -\frac{1}{r^2} \qquad O\left(\frac{1}{r^2}\right),\ r \to \infty$$

$$\frac{d^2G}{dr^2} = \frac{2}{r^3} \qquad O\left(\frac{1}{r^3}\right),\ r \to \infty$$

$$\frac{d^3G}{dr^3} = -\frac{6}{r^4} \qquad O\left(\frac{1}{r^4}\right),\ r \to \infty$$

Dynamic Source.
e.g. Hertian dipole

$$G = \frac{e^{ikr}}{r}$$

$$\frac{dG}{dr} \sim ik\frac{e^{ikr}}{r} \qquad O\left(\frac{1}{r}\right),\ r \to \infty$$

$$\frac{d^2G}{dr^2} \sim k^2\frac{e^{ikr}}{r} \qquad O\left(\frac{1}{r}\right),\ r \to \infty$$

$$\frac{d^3G}{dr^3} \sim -ik^3\frac{e^{ikr}}{r} \qquad O\left(\frac{1}{r}\right),\ r \to \infty$$

EVANESCENT AND PROPAGATING WAVES

- Angular spectral plane wave decomposition of the free space Green's function
- Propagating waves and evanescent waves contribute to the final field

$$\begin{aligned}\frac{e^{ik|\mathbf{D}+\mathbf{d}|}}{|\mathbf{D}+\mathbf{d}|} &= \frac{ik}{2\pi}\int_{\Gamma} d\theta \int_0^{2\pi} d\phi \, \sin(\theta) e^{i\mathbf{k}\cdot\mathbf{d}} e^{i\mathbf{k}\cdot\mathbf{D}} \\ &= \mathcal{G}_1 + \mathcal{G}_2 + \mathcal{G}_3.\end{aligned}$$

$$\mathcal{G}_n = \frac{ik}{2\pi}\int_{\Gamma_n} d\theta \int_0^{2\pi} d\phi \, \sin(\theta) e^{i\mathbf{k}\cdot\mathbf{d}} e^{i\mathbf{k}\cdot\mathbf{D}} \quad n = 1, 2, 3$$

EVANESCENT AND PROPAGATING WAVES

- Integration path can be divided into three segments.
- Plane waves are therefore categorized into three kinds

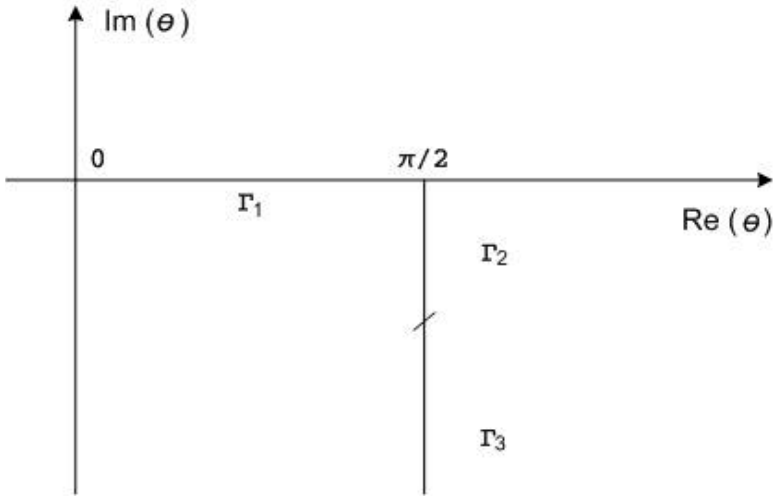

$\mathcal{G}_1$ **Propagating Waves**

$\mathcal{G}_2$ **Shallow Evanescent Waves**

$\mathcal{G}_3$ **Deep Evanescent Waves**

- Evanescent waves on Γ_3 are less significant when it goes to $-i\infty$
- Truncation of Γ_3 determines the accuracy

DIRECTION DEPENDENCE

- Propagating waves can be accurately computed
- Evanescent waves can be truncated
- Both kinds of waves are direction dependent

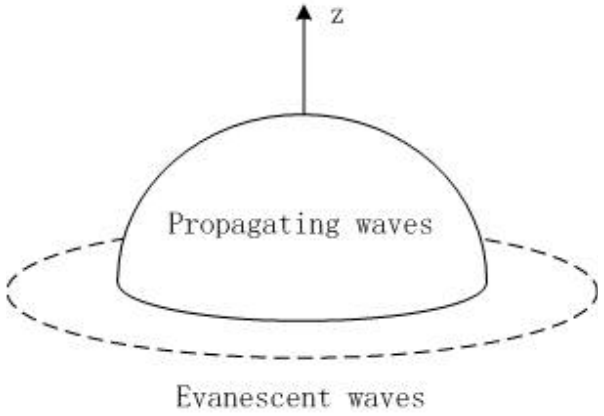

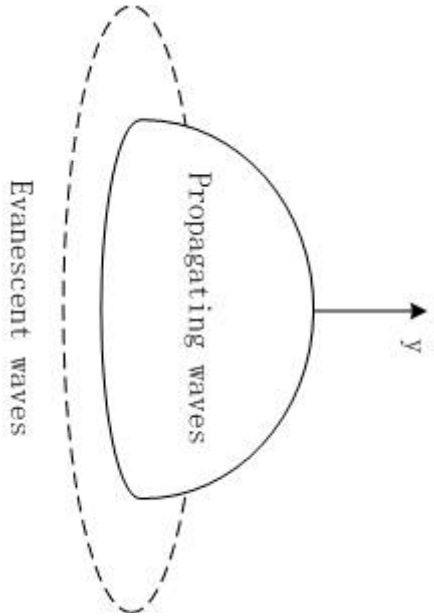

SHALLOW EVANESCENT WAVES

- The evanescent waves close to the real axis (*shallow evanescent waves*) can be extrapolated
- The shareable propagating wave data can be used to represent shallow evanescent waves

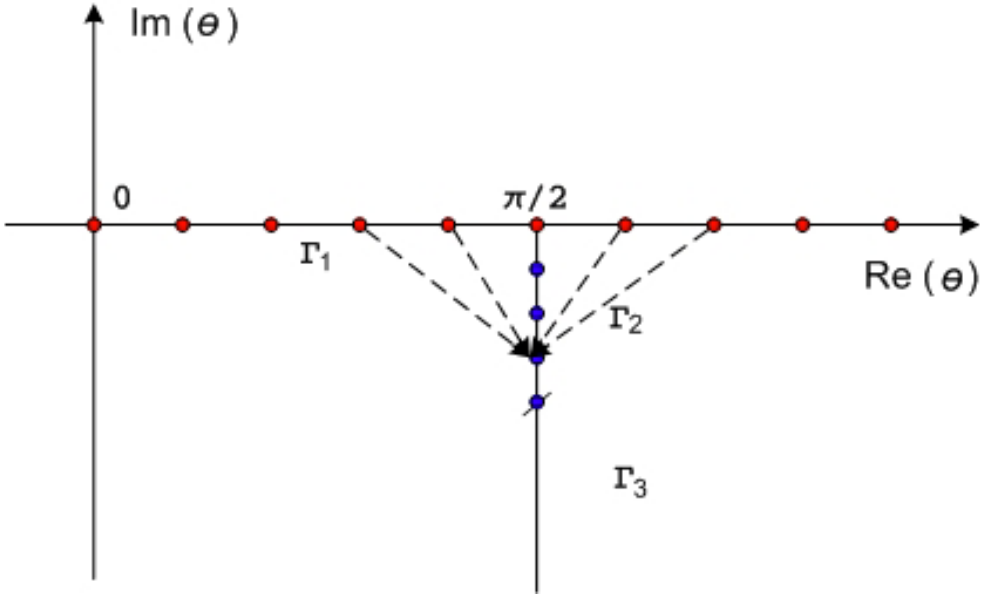

SHALLOW EVANESCENT WAVES

- The resultant translators can be merged into the propagating wave translators
- High frequency evanescent waves and normal propagating waves are manipulated by one set of propagating wave data on a sphere

$$\mathcal{T}_{prop}(\theta_{sp}, \phi_{sp}) = \mathcal{T}_{p}(\theta_{sp}, \phi_{sp}) + \mathcal{T}_{pe}(\theta_{sp}, \phi_{sp})$$

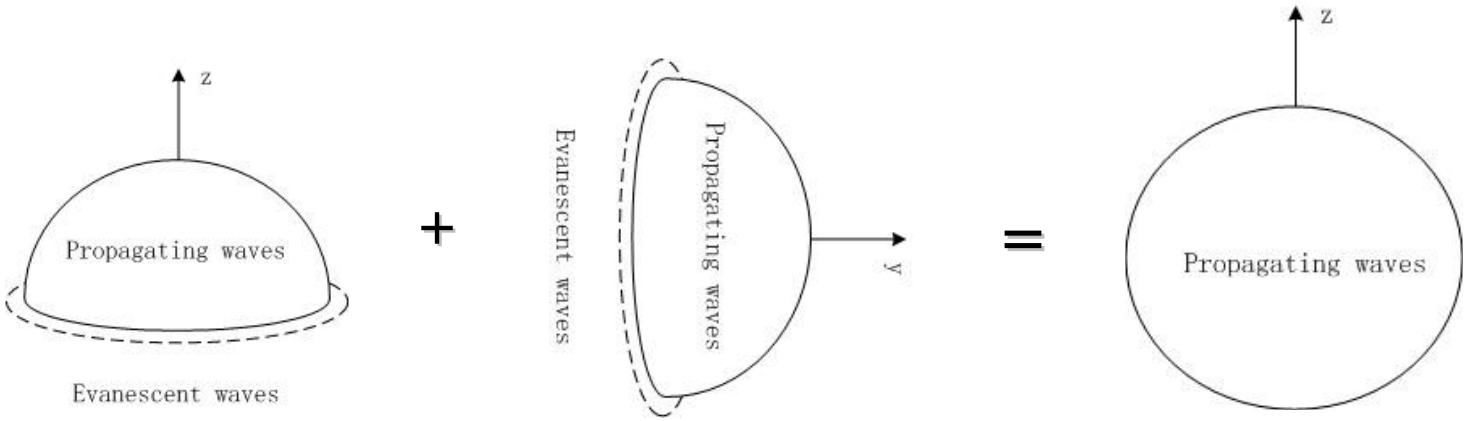

DEEP EVANESCENT WAVES

- The residual evanescent waves (*deep evanescent waves*) have to be stored, especially for the low frequency case
- At high frequencies, this part will automatically disappear due to its decaying property

$$
\begin{aligned}
\mathcal{G}_3 &= \frac{1}{2\pi}\int_{\sigma_o}^{+\infty} d\sigma \int_0^{2\pi} d\phi\, e^{i\mathbf{k}\cdot\mathbf{d}} e^{i\mathbf{k}\cdot\mathbf{D}} \\
&= \sum_{\theta_{se}}\sum_{\phi_{se}} e^{i\mathbf{k}\cdot\mathbf{d}}(\theta_{se},\phi_{se}) \cdot \{w_{\theta_{se}} w_{\phi_{se}} e^{i\mathbf{k}\cdot\mathbf{D}}(\theta_{se},\phi_{se})\} \\
&= \sum_{\theta_{se}}\sum_{\phi_{se}} e^{i\mathbf{k}\cdot\mathbf{d}}(\theta_{se},\phi_{se}) \cdot \mathcal{T}_e(\theta_{se},\phi_{se}).
\end{aligned}
$$

MULTIPOLE EXPANSION

$$\bar{\boldsymbol{\alpha}}_{LL'}(\mathbf{r}_{ji}) = \bar{\boldsymbol{\beta}}_{LL_1}(\mathbf{r}_{jJ}) \cdot \bar{\boldsymbol{\alpha}}_{L_1L_2}(\mathbf{r}_{JI}) \cdot \bar{\boldsymbol{\beta}}_{L_2L'}(\mathbf{r}_{Ii})$$

$$\bar{\boldsymbol{\alpha}}_{LL'}(\mathbf{r}_{ji}) = \left(\frac{1}{t}\right)^{l} \left[\beta^N_{LL_0} \left(\frac{t}{t_0}\right)^{l_0}\right] \left[\beta^N_{L_0L_1} \left(\frac{t_0}{t_1}\right)^{l_1}\right] \left[\alpha^N_{L_1L_2} \left(\frac{1}{t_1}\right)\right] \left[\left(\frac{t_2}{t_1}\right)^{l_2} \beta^N_{L_2L_3}\right] \left[\left(\frac{t'}{t_2}\right)^{l_3} \beta^N_{L_3L'}\right] \left(\frac{1}{t'}\right)^{l'}$$

$$\alpha_{00}(\mathbf{r}_{ji}) = \left[\beta^N_{0L_0} \left(\frac{1}{2}\right)^{l_0}\right] \left[\beta^N_{L_0L_1} \left(\frac{1}{2}\right)^{l_1}\right] \left[\alpha^N_{L_1L_2} \left(\frac{1}{t_1}\right)\right] \left[\left(\frac{1}{2}\right)^{l_2} \beta^N_{L_2L_3}\right] \left[\left(\frac{1}{2}\right)^{l_3} \beta^N_{L_30}\right]$$

- The point source is expanded into multipoles by the addition theorem
- Normalization is needed at very low frequencies to achieve O(1) magnitude in the leading term of multipole expansions
- Oct-tree is used and dense translations have a cost of $(P+1)^4$ or $(P+1)^3$ if P is the multipole truncation number

ERRORS OF MULTIPOLE EXPANSIONS

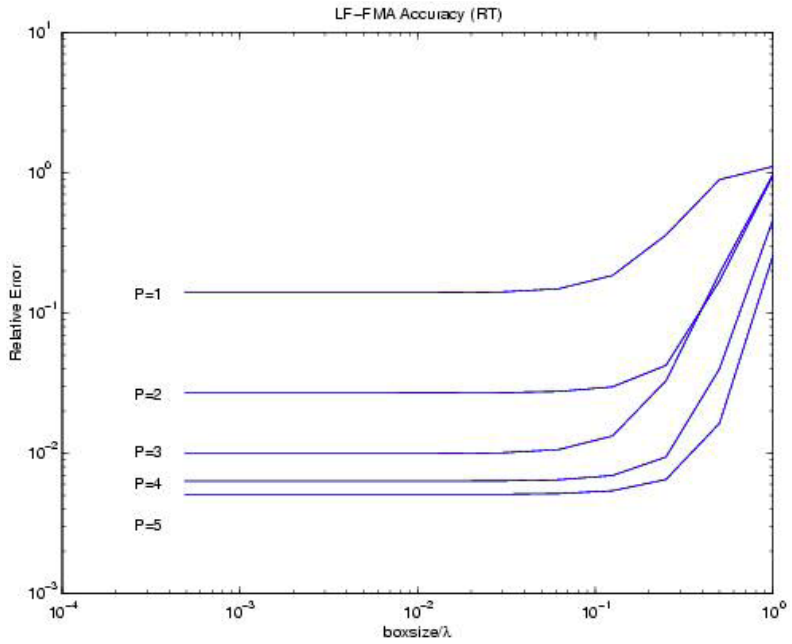

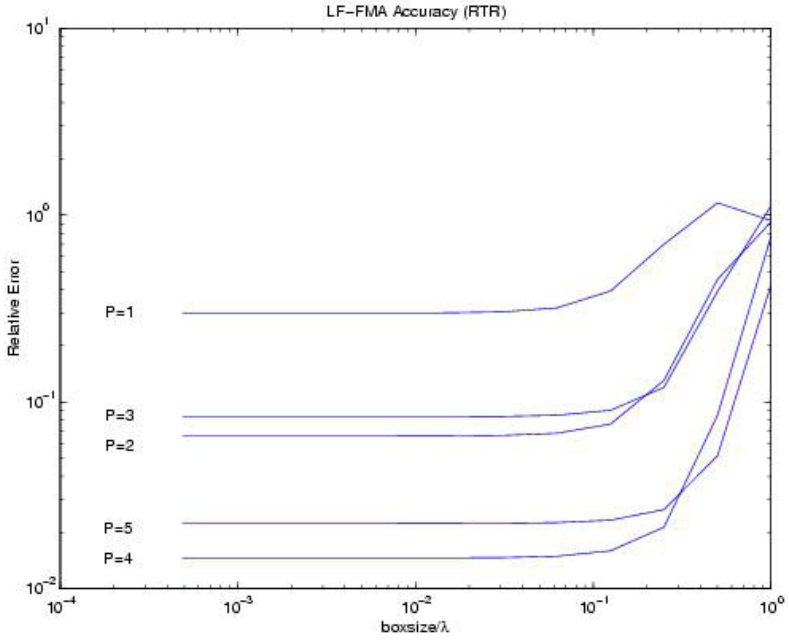

- The accuracy drops sharply after 0.2λ
- More multipoles have low efficiency in improving the accuracy
- Dense matrix translation makes the algorithm not efficient

ERRORS of PLANE WAVE REPRESENTATION

$$\mathcal{T}_L(\mathbf{k},\mathbf{D}) = \sum_{l=0}^{L} i^l(2l+1)h_j^{(1)}(kD)P_l(\hat{k}\cdot\hat{D})$$

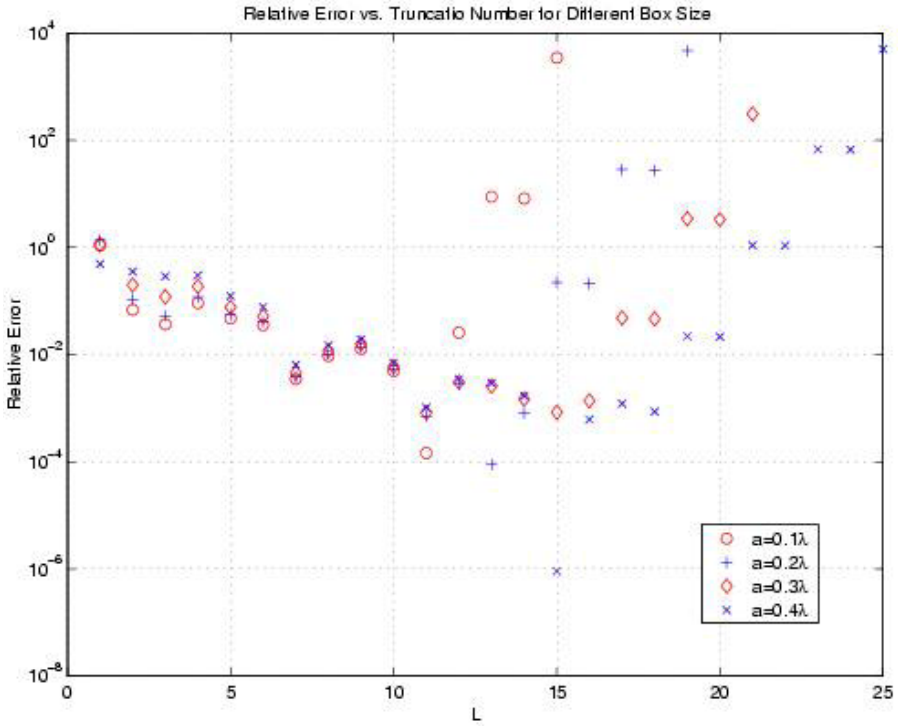

- The accuracy drops below 0.2λ
- An optimized mode number L is required to achieve the best possible accuracy
- Several percent error could be obtained

$$L \approx kd + 1.8d_0^{2/3}(kd)^{1/3}$$

MULTIPOLE TO PLANE WAVE

$$
\begin{aligned}
\left[\alpha_{LL'}(\mathbf{r}_{ji})\right]_{L\times L'} = {} & \left[\beta_{LL_1}(\mathbf{r}_{jJ_1})\right]_{L\times L_1} && \text{Low frequency}\\
\cdot\ & \left[\beta_{L_1L_2}(\mathbf{r}_{J_1J_2})\right]_{L_1\times L_2}\cdot\left[\beta_{L_2L_3}(\mathbf{r}_{J_2J_3})\right]_{L_2\times L_3} && \\
\cdot\ & [D]^{\dagger}_{S_4\times L_3} && \text{Transformer}\\
\cdot\ & \text{diag}\left[e^{i\mathbf{k}\cdot\mathbf{r}_{J_3J_4}}\right]_{S_4\times S_4}\cdot[I]^{T}_{S_5\times S_4} && \\
\cdot\ & \text{diag}\left[e^{i\mathbf{k}\cdot\mathbf{r}_{J_4J_5}}\right]_{S_5\times S_5} && \\
\cdot\ & \text{diag}\left[\tilde{\mathcal{T}}(\Omega_{s_5},\mathbf{r}_{J_5I_5})w_{s_5}\right]_{S_5\times S_5} && \text{Mid frequency}\\
\cdot\ & \text{diag}\left[e^{i\mathbf{k}\cdot\mathbf{r}_{I_5I_4}}\right]_{S_5\times S_5}\cdot[I]_{S_5\times S_4} && \\
\cdot\ & \text{diag}\left[e^{i\mathbf{k}\cdot\mathbf{r}_{I_4I_3}}\right]_{S_4\times S_4} && \\
\cdot\ & [D]_{S_4\times L_3} && \text{Transformer}\\
\cdot\ & \left[\beta_{L_3L_2}(\mathbf{r}_{I_3I_2})\right]_{L_3\times L_2}\cdot\left[\beta_{L_2L_1}(\mathbf{r}_{I_2I_1})\right]_{L_2\times L_1} && \\
\cdot\ & \left[\beta_{L_1L'}(\mathbf{r}_{I_1i})\right]_{L_1\times L'} && \text{Low frequency}
\end{aligned}
$$

FULL BAND SIMULATION USING MULTIPOLES AND PLANE WAVES

$r = 1.0$ meter sphere. 0.12GHz. 3 level mixed-form FMA. 2 multipole translation levels. Leafy box size is 0.05λ. 24576 RWGs.

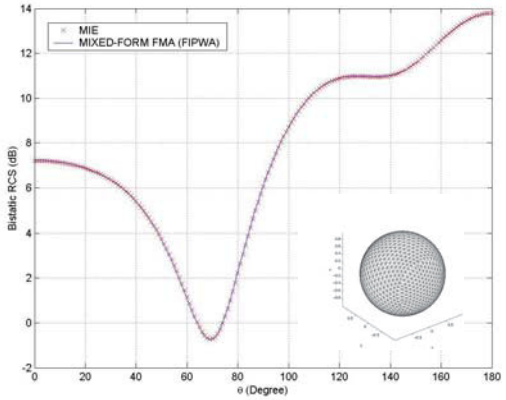

$r = 1.0$ meter sphere. 0.24GHz. 3 level mixed-form FMA. 2 diagonal translation levels. Leafy box size is 0.1λ. 24576 RWGs.

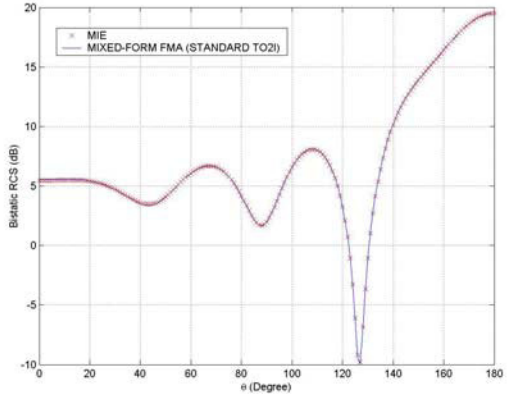

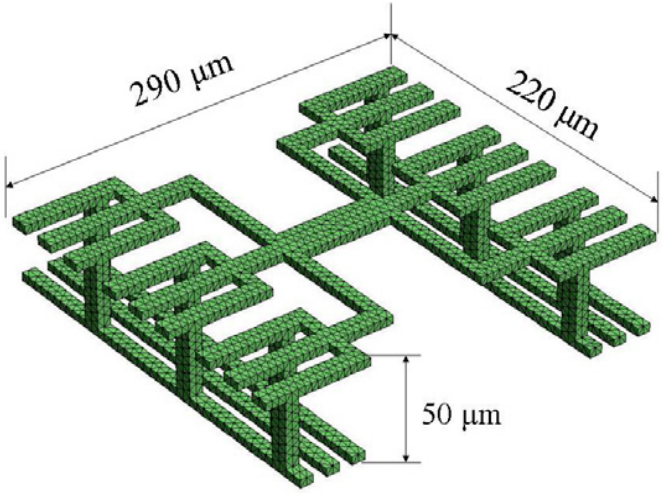

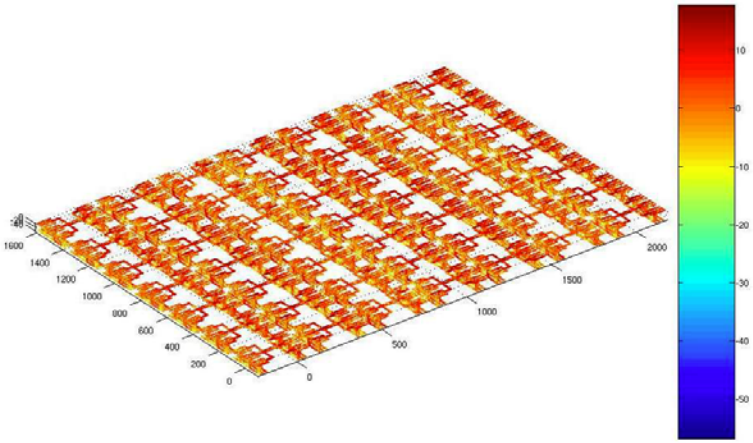

STATIC SOLVERS AND FULL WAVE SOLVERS

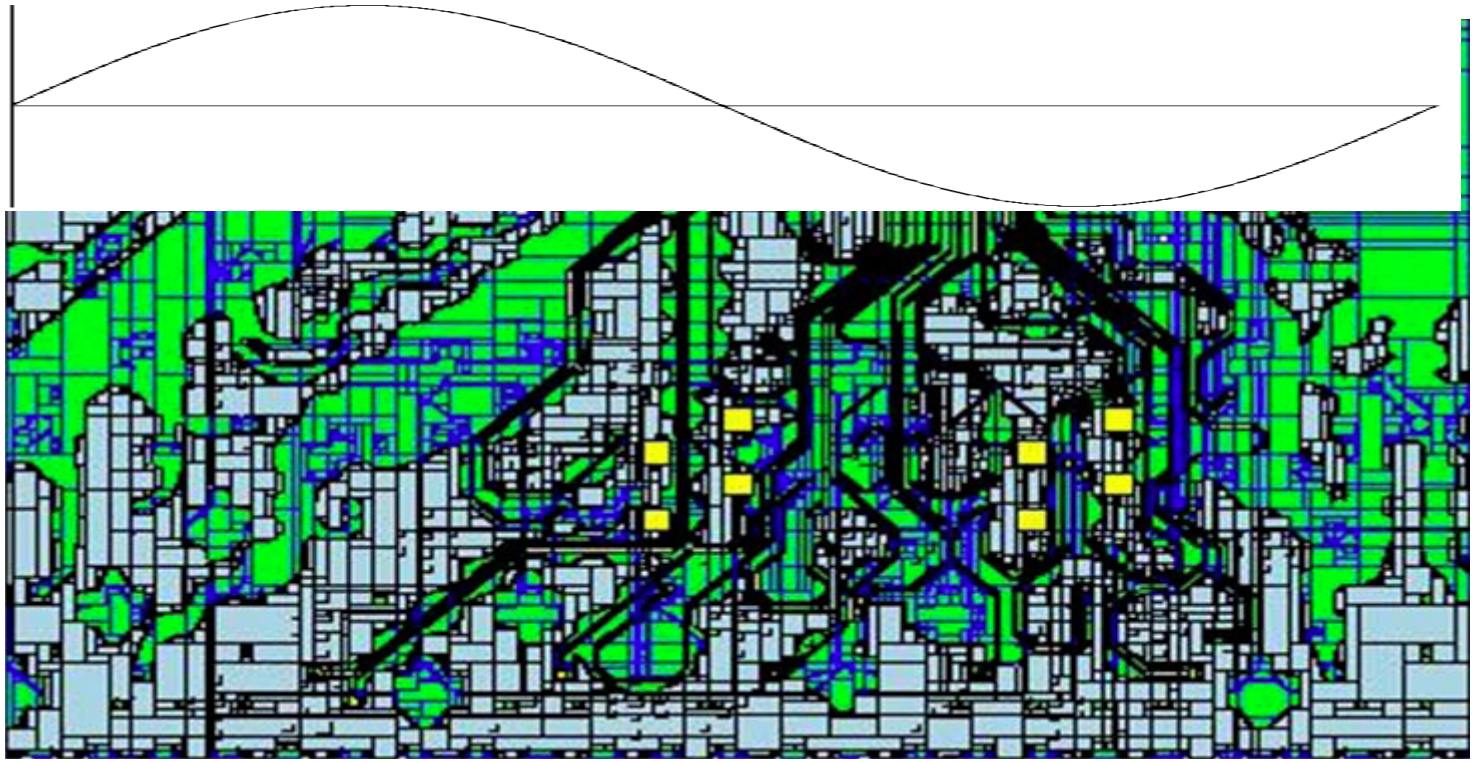

Static analysis, quasi static parasitic parameter extraction

Circuit theories or circuit analogy solvers will work correctly

Full wave analysis, circuit approximation will not be a reliable Choice.

LF ALGORITHMS AND HF ALGORITHMS

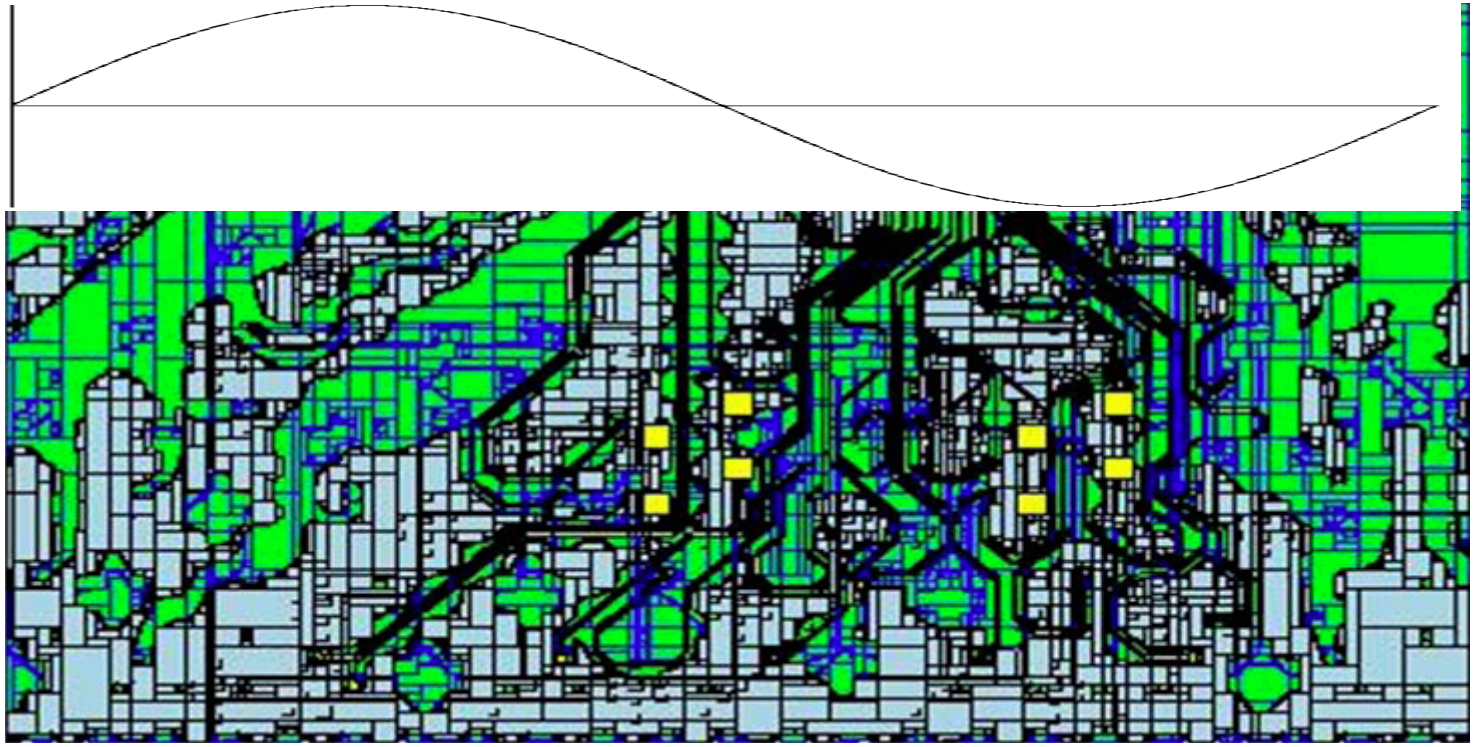

QR decomposition, SVD, Pre-corrected FFT, LFFMA will work.

MLFMA, Ray Tracing, and GO will work.

SHORT SUMMARY

- **Multiscale problem is more than the computing capacity issue. It is a multi-physics problem in terms of frequency.**
- **Wave physics are altering vs frequencies.**
- **Electric field and magnetic field coupling features cause two different types of numerical analysis difficulties.**
- **Proper strategies shall be taken to deal with complicated on-chip and packaging problems.**
- **Both first principle solvers and their algorithms shall be taken into account to guarantee a meaningful SI simulation result.**

OUTLINES

- **Multi-physics vs. Frequencies**
  - Helmholtz Decomposition
  - Evanescent Waves and Propagating Waves
  - Algorithm Dependencies
- **Multi-physics Thermal Electrical Coupling Analysis**
  - Thermal Conduction Modeling
  - Novel Equivalent Thermal Conductivity Calculation
  - Thermal Guideline Study
  - Thermal-electrical Coupling Simulation
- **Conclusions**

THERMAL EFFECTS

- **Self-heating or Joule heating caused by current flow in interconnects.**
- **Main impact will be Electromigration (EM) Reliability**
- **Thermal effects are increasing with scaling, due to:**
  - Higher power-densities and more metal layers on the chip
  - Shrinking BEOL dimensions
  - 3D Integration
  - Use of low-k dielectric materials (also have low thermal conductivity)
  - Thermally poor device technologies like SOI, strained silicon etc.
- **Existing tools are powerful, sophisticated, and expensive**
- **Our motivation is**
  - use existing tools to answer the thermal questions
  - enable embedded thermal analysis for internal tools and processes
  - make it very easy to use

ANALOGY BETWEEN CURRENT CONDUCTION AND HEAT CONDUCTION

Poisson's Equation

$\nabla(\varepsilon\nabla\phi) = -\rho$

In the dielectric (Im. Part):

$\nabla(\sigma_{el}\nabla\phi) = 0$

Electrical Current Density:

$$\frac{I}{A} = J = \sigma_{el}E = -\sigma_{el}\frac{\partial\phi}{\partial x}$$

Heat Equation (Steady-State):

$\nabla(\kappa_{th}\nabla T) = -q'''_g$

In the dielectric (No heat generation):

$\nabla(\kappa_{th}\nabla T) = 0$

Thermal Flux:

$$\frac{q}{A} = \Phi_{th} = -\kappa_{th}\frac{\partial T}{\partial x}$$

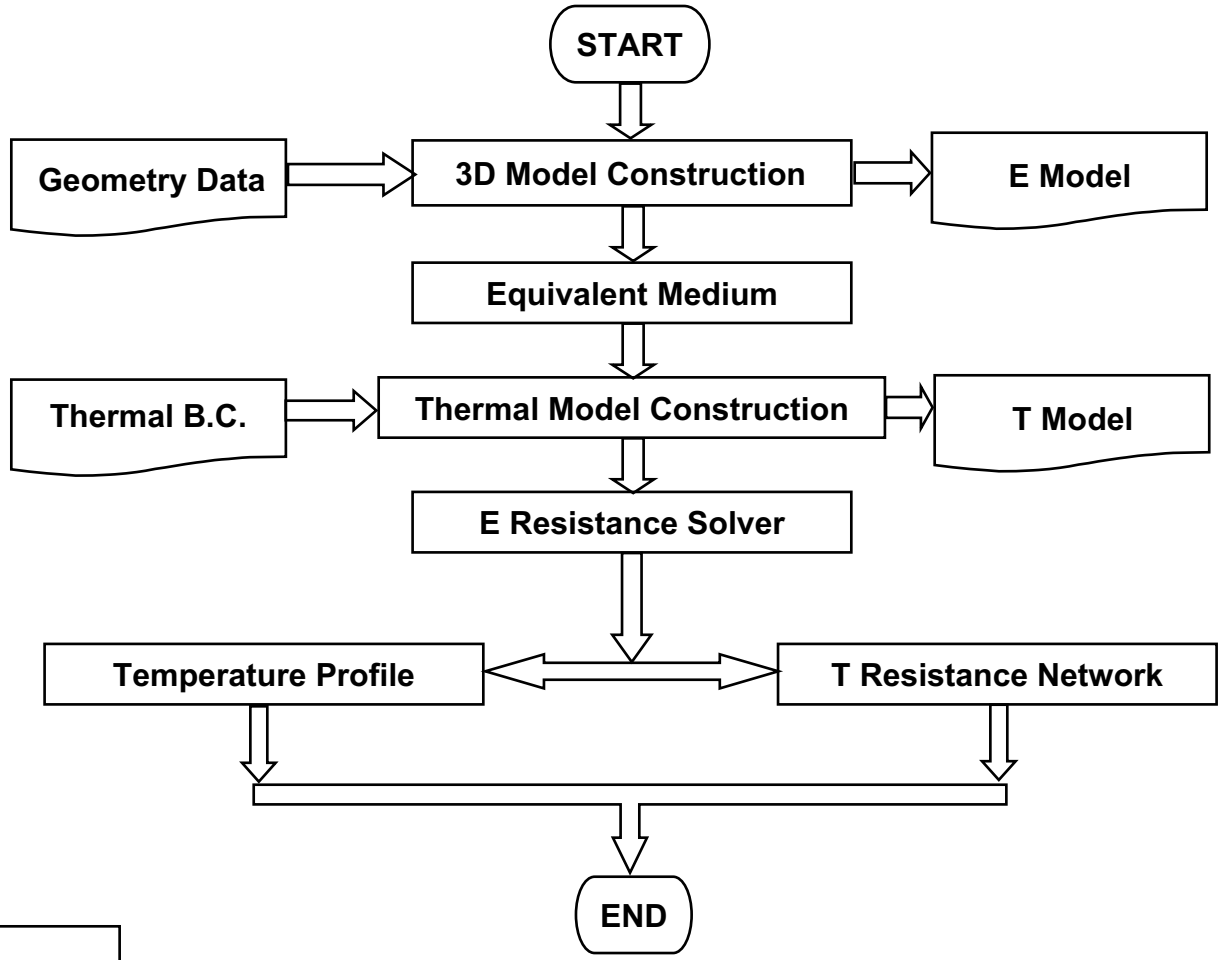

Potential (ϕ) $\Leftrightarrow$ Temperature (T)

Current (I) $\Leftrightarrow$ Heat Flow (q)

Elec. Conductivity (σ_{el}) $\Leftrightarrow$ Thermal Conductivity (κ_{th})

Elec. Resistance (R_{el}) $\Leftrightarrow$ Thermal Resistance (R_{th})

- **Both electrical and thermal resistance problems are using similar Laplace's equations.**
- **An electrical resistance solver can serve as the thermal conduction solver.**
- **IBM EIP/EDA RGEN/RSURF is used as the resistance solver.**

FINITE DIFFERENCE SOLVER

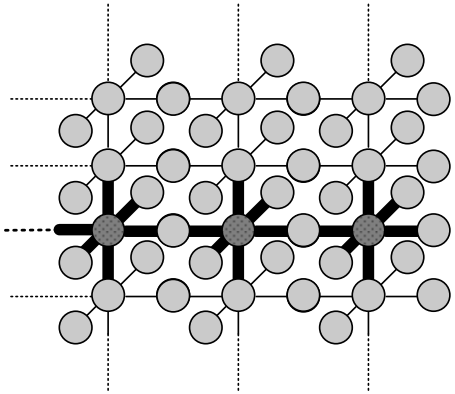

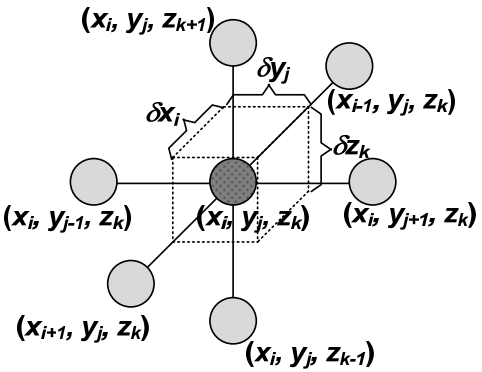

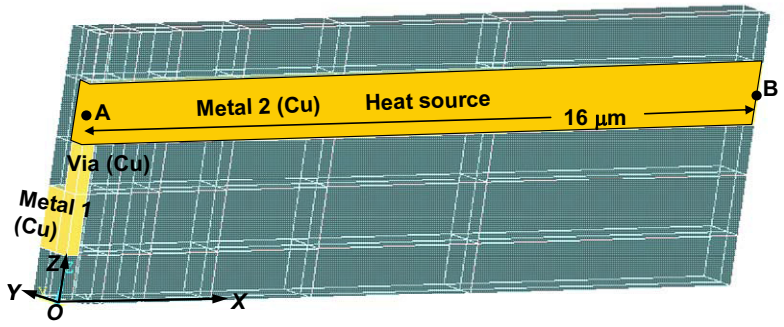

KCL is used

$$G_{i+,j,k}=\frac{1}{4}\Big[\sigma_{i+,j+,k+}\left(y_{j+1}-y_j\right)\left(z_{k+1}-z_k\right)$$
$$+\sigma_{i+,j-,k+}\left(y_j-y_{j-1}\right)\left(z_{k+1}-z_k\right)+\sigma_{i+,j-,k-}\left(y_j-y_{j-1}\right)\left(z_k-z_{k-1}\right)$$
$$+\sigma_{i+,j+,k-}\left(y_{j+1}-y_j\right)\left(z_k-z_{k-1}\right)\Big]\Big/\left(x_{i+1}-x_i\right)$$
$$G_{i+,j,k}\left(V_{i+1,j,k}-V_{i,j,k}\right)+G_{i-,j,k}\left(V_{i-1,j,k}-V_{i,j,k}\right)$$
$$+G_{i,j+,k}\left(V_{i,j+1,k}-V_{i,j,k}\right)+G_{i,j-,k}\left(V_{i,j-1,k}-V_{i,j,k}\right)$$
$$+G_{i,j,k+}\left(V_{i,j,k+1}-V_{i,j,k}\right)+G_{i,j,k-}\left(V_{i,j,k-1}-V_{i,j,k}\right)=-\delta I_{i,j,k}$$

	C-Tool	CHIPJOULE (G = 3)	Error
T_B (K)	22.943	22.871	-0.31%
DT_B-DT_A (K)	1.677	1.684	0.45%

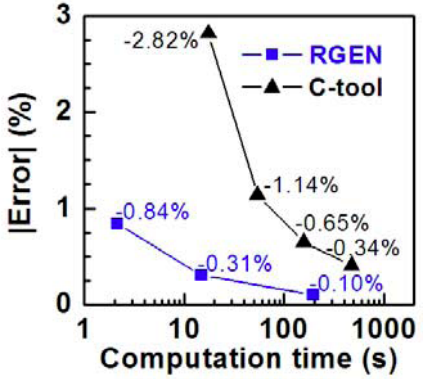

ANISOTROPIC MEDIUM

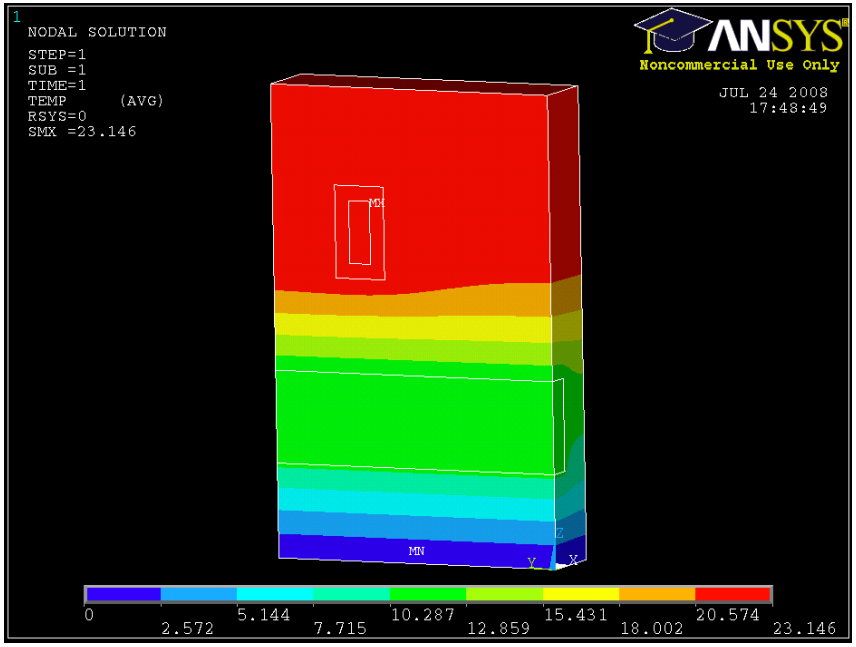

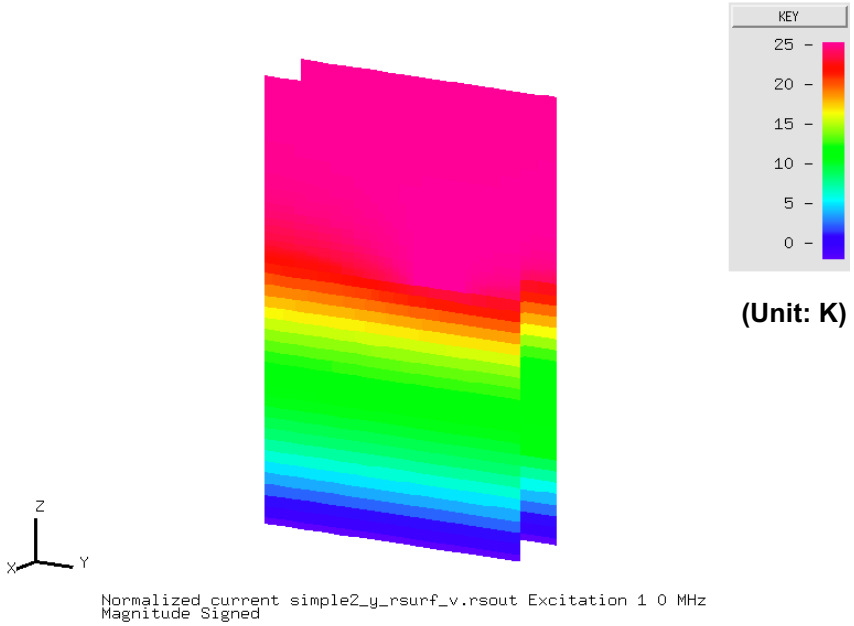

Temperature Profile Obtained From 3D-ANSYS and CHIPJOULE

	ANSYS (K)	CHIPJOULE (K)
Isotropic Dielectric ($K = K_0$ = 0.8 W/m-K)	26.529	26.432 -0.36%
Anisotropic Dielectric ($K_y = K_z = 0.1K_x = K_0$)	24.995	24.967 -0.11%
Anisotropic Dielectric ($K_x = K_z = 0.1K_y = K_0$)	23.146	23.152 +0.03%
Anisotropic Dielectric ($K_x = K_y = 0.1K_z = K_0$)	3.9393	3.9433 +0.10%

VARIOUS ON CHIP STRUCTURES

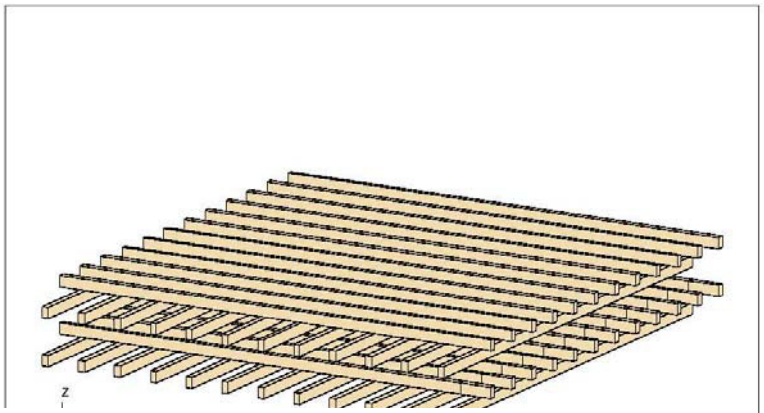

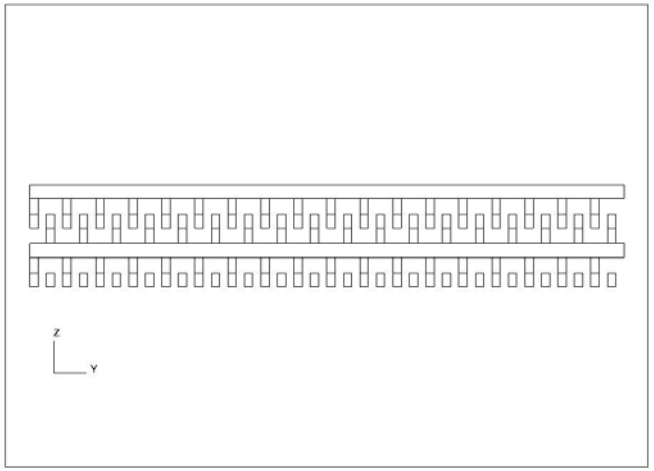

Collaboration with Evan Colgan (YKT), Jamil Wakil (STG, Austin)

EMPIRICAL APPROACH BASED ON ELECTRO-THERMAL ANALOG

$$\frac{C}{\epsilon} = \frac{W}{H} + 1.086\left(1 + 0.685e^{\frac{-T}{1.343S}} - 0.9964e^{\frac{-S}{1.421H}}\right) \cdot \left(\frac{S}{S+2H}\right)^{0.0476}\left(\frac{T}{H}\right)^{0.337}$$

G_{th}/K_{th}

Valid for $0.3 \le W/H \le 10, 0.3 \le S/H \le 10$

- Assuming stratified medium with no vacuum or air gaps existing in the interested region. All fields are contained within the medium.
- Capacitance analog works for thermal analysis
- Capacitive coupling is analog of the thermal conductance
- Transmission line coupling effects are considered.

[4] J.-H. Chern, et al, "Multilevel Metal Capacitance Models For CAD Design Synthesis Systems," EDL, Vol. 13, No. 1, Jan. 1992.

COMPARISON BETWEEN DIFFERENT ANALYTICAL AND EMPIRICAL MODELS (NO VIAS)

Kdiel (W/mK)	Kmetal (W/mK)	Llines (um)	Lvias (um)	No. of IMDs	No. of ILDs	Wlines (um)	Wvias (um)
0.54	380	0.475	0.525	4	4	0.28	0.28

Thermal Resistance in unit Area (K-mm^2/W) and % error w.r.t. ANSYS

	Line density = 0.5	Line density = 0.167
ANSYS	4.1	5.7
Chiang [2]	4.69 (14.4%)	13.14 (130.5%)
Im [3]	3.90 (-4.9%)	3.92 (-31.3%)
Our Method	3.97 (-3.2%)	6.26 (9.8%)

[1] T.-Y. Chiang, K. Banerjee, and K. C. Saraswat, “Analytical Thermal Model for Multilevel VLSI Interconnects Incorporating Via Effect,” EDL, Vol. 23, No. 1, Jan. 2002.

[2] S. Im, N. Srivastava, K. Banerjee, and et al, “Scaling Analysis of Multi-level Interconnect Temperatures for High-Performance ICs,” TED, Vol. 52, No. 12, Dec. 2005.

COMPARISON BETWEEN DIFFERENT ANALYTICAL AND EMPIRICAL MODELS (WITH STACKED VIAS)

Im's Model [2]: $R_{th} = R_{th,no\text{-}vias} \,||\, N_{vias}R_{via}$

Proposed Model: $R_{th} = R_{th,no\text{-}vias} \,||\, (N_{vias}R_{via} + R_{line}/4)$

K_{diel} (W/mK)	K_{metal} (W/mK)	L_{lines} (um)	L_{vias} (um)	No. of IMDs	No. ILDs with vias	No. ILDs w/o. vias	W_{lines} (um)	W_{vias} (um)
0.54	380	0.475	0.525	4	3	1	0.28	0.28

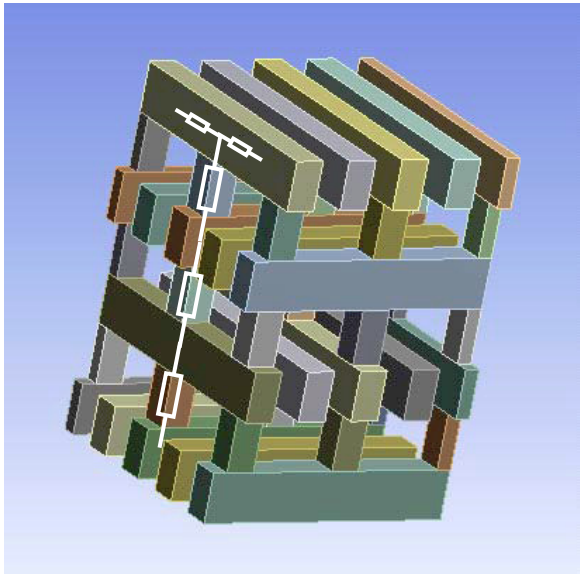

Thermal Resistance in unit Area (K-mm^2/W) (Line density = 0.5)

	Via density = 0	Via density = 0.0031	Via density = 0.0625
ANSYS	4.1	2.9	1.2
Im [2]	3.90 (-4.9%)	1.90 (-34.5%)	1.05 (-12.5%)
Proposed Model	3.97 (-3.2%)	3.05 (5.2%)	1.12 (-6.7%)

ON-CHIP THERMAL GUIDELINE STUDY

10x – 2 mm
4x – 1 mm
2x - 0.5 mm
1.25x – 0.25 mm

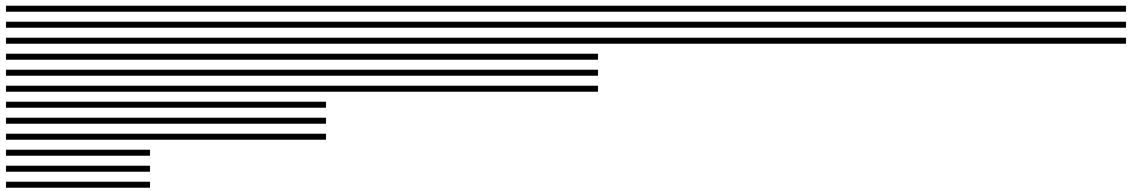

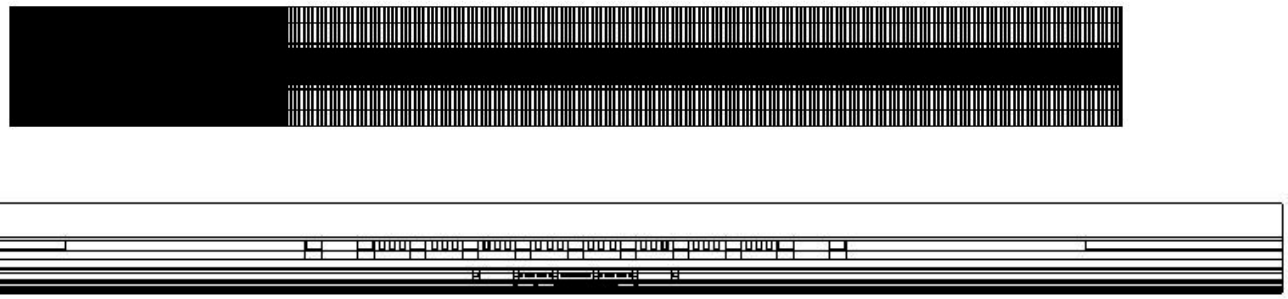

12K bodies – Layers 4 – 11, signal lines on layers 5, 7, 9, 11
with vias between power conductors, orthogonal power on layers 4, 6, 8, 10

Based on discussions with Howard Smith. Created by Alina Deutsch.

SIMPLIFICATION OF THE STACK

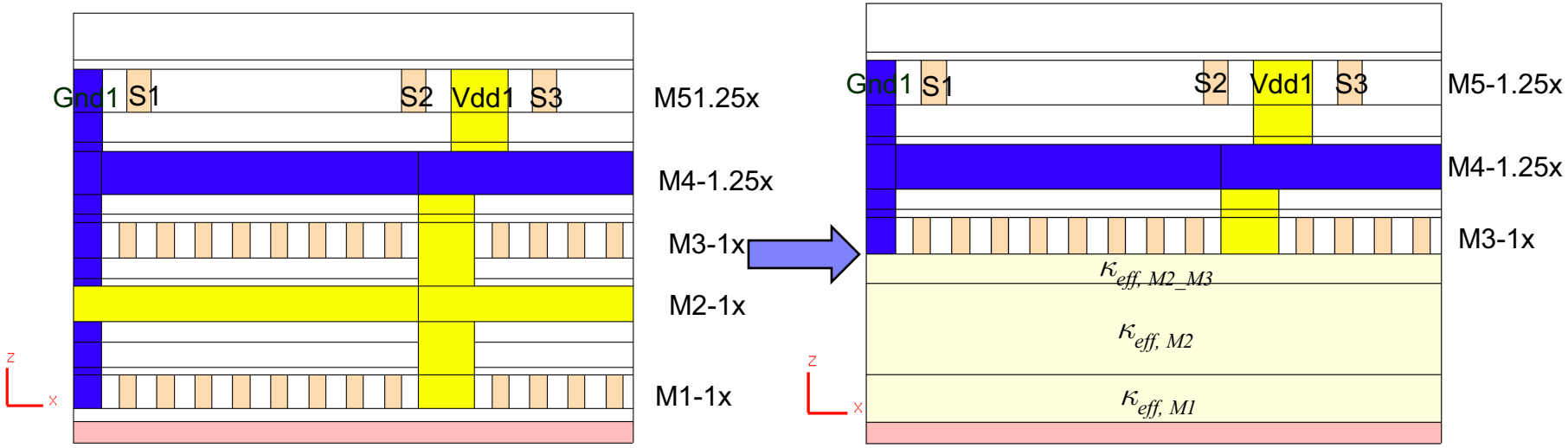

Use the proposed empirical model to extract thermal conductance per unit length (G_{th,no_via}) in each layer (not including via effect, using average wire width and/or spacing);

$$\kappa_{eff,\ no\_via} = G_{th,\ no\_via}\,(t+h)/(w+s);$$

$$\kappa_{eff} = \kappa_{eff,\ no\_via}(1-ViaDensity)+\kappa_{via}ViaDensity$$

$I = 1$ mA in S1, S2 and S3 Gridding level = 2

SIMPLIFICATION OF THE STACK

	X1	Y1	Z1	X2	Y2	Z2	Full Stack	Only M3~M5	error%
$T_{avg,\ Gnd1}$ (K)	0.000	0.000	1.436	0.000	18.240	1.436	1.2362	1.2200	**-1.3%**
$T_{avg,\ S1}$ (K)	0.266	0.000	1.436	0.266	18.240	1.436	1.6507	1.6297	**-1.3%**
$T_{avg,\ S2}$ (K)	1.386	0.000	1.436	1.386	18.240	1.436	1.6573	1.6403	**-1.0%**
$T_{avg,\ Vdd1}$ (K)	1.652	0.000	1.436	1.652	18.240	1.436	1.2494	1.2407	**-0.7%**
$T_{avg,\ S3}$ (K)	1.918	0.000	1.436	1.918	18.240	1.436	1.6875	1.6707	**-1.0%**
$T_{avg,\ C2}$ (K)	0.000	0.000	1.436	2.280	18.240	1.436	1.3833	1.3643	**-1.4%**
$T_{avg,\ C1}$ (K)	0.000	0.000	1.101	2.280	18.240	1.101	0.9371	0.9116	**-2.7%**
$\Delta T_{S1,Gnd1}$							0.4145	0.4096	**-1.2%**
$\Delta T_{S2,Vdd1}$							0.4079	0.3996	**-2.0%**
$\Delta T_{S3,Vdd1}$							0.4381	0.4300	**-1.9%**
$\Delta T_{C2,C1}$							0.4462	0.4527	**1.5%**
Computation time							**5.8 h**	**50 min**	

8 WIRE JOULE HEATING

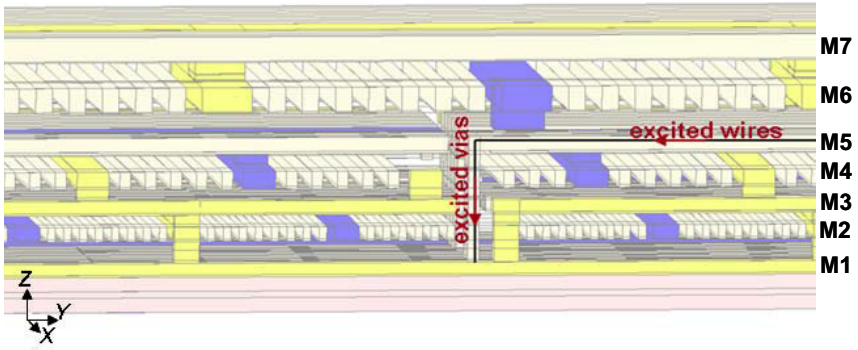

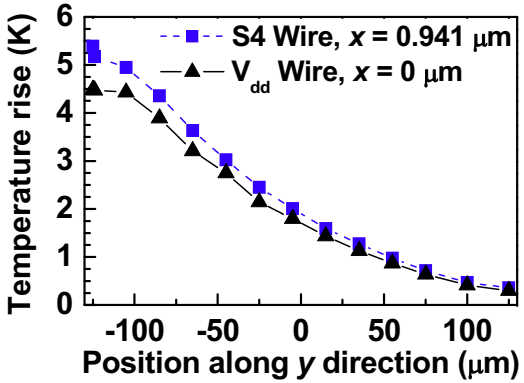

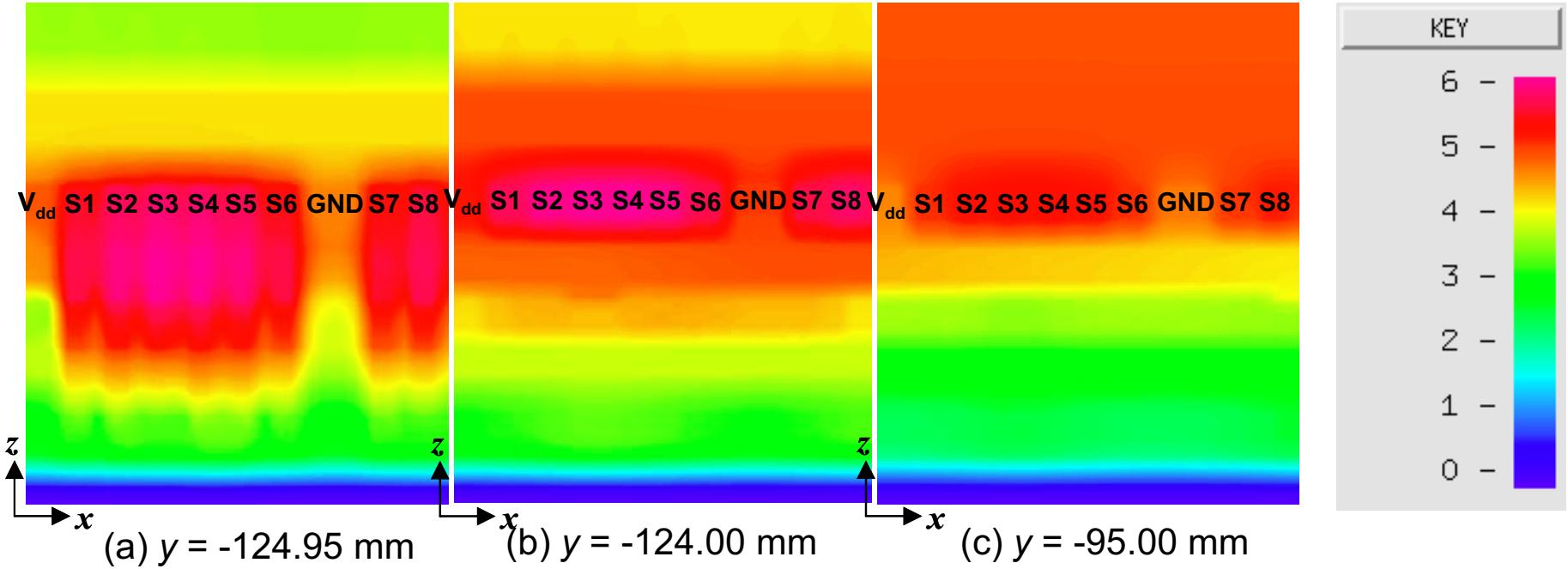

(a) y = -124.95 mm (b) y = -124.00 mm (c) y = -95.00 mm

IBM_GIT CHIPJOULE THERMAL-ELECTRICAL COUPLING SIMULATION PROJECT

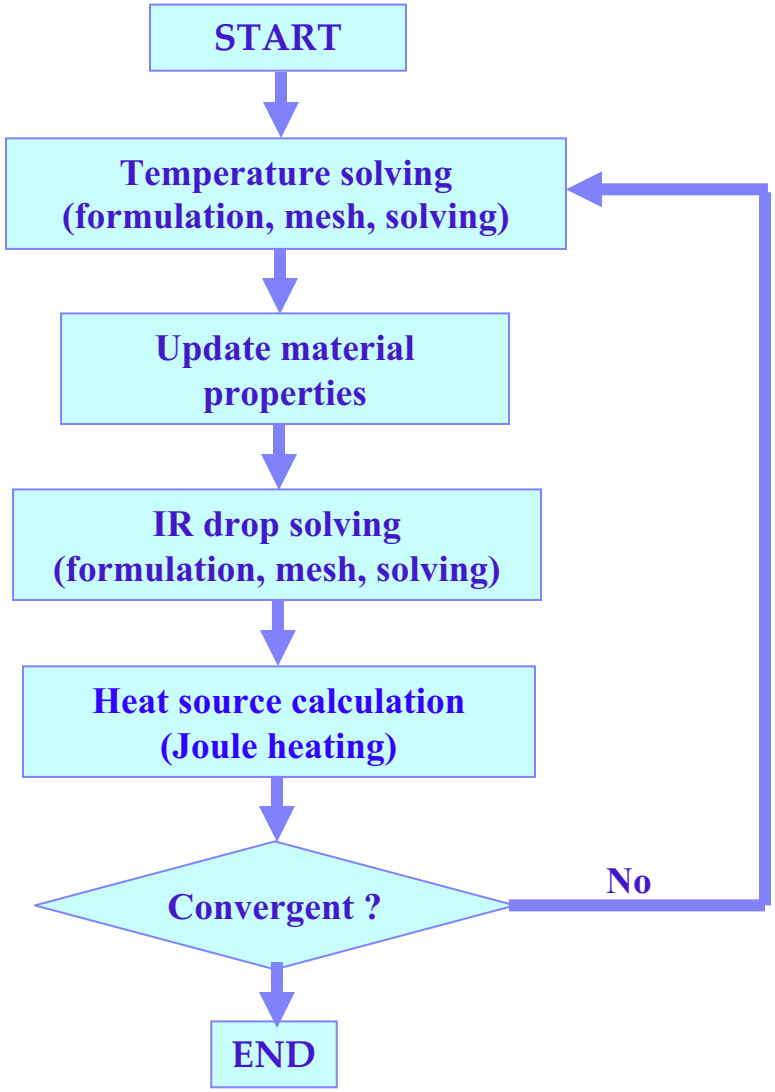

Procedure:

- Temperature distribution solving based on initial thermal conditions (**chipJoule**).
- Update the temperature distribution profiles to every location of conductors in PDN.
- Voltage distribution solving based on the temperature profile (**Rgen**).
- Ohmic loss (Joule heating) calculation from the power density distribution **(Rgen)**
- Judge whether convergence or not? If convergent, stop and output results; If not, go to next step. (first iteration is enabled)
- New temperature distribution solving based on the thermal condition plus the new heat source from electrical field **(chipJoule).**
- Do close-loop iteration from step 2-6.

SIMULATION SETUP FOR 3D STACKED CHIPS BY GIT FOR IBM-GIT PROJECT

1. C4 balls are added between two stacked chips
2. C4 balls are also added between bottom chip and substrate.
3. C4 balls are converted to pillars in the simulation.
4. The material of C4 is Sn-0.7Cu alloy.
5. The total area occupied by C4 is 50% of the interface area (assumption).
6. At chip area, the power distribution is non-uniform (shown in next page).

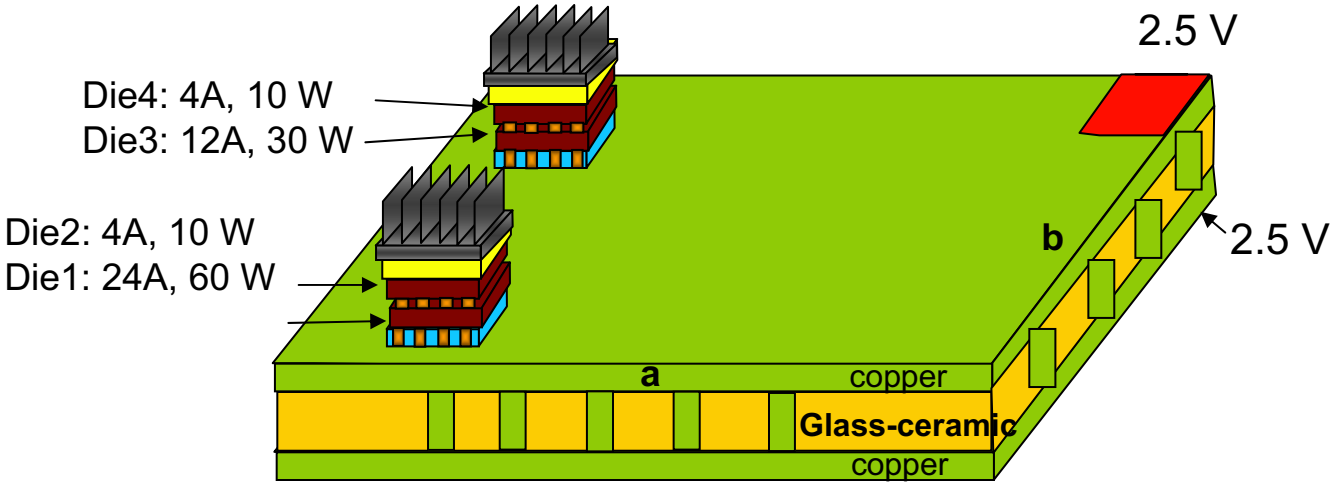

Cross section view:

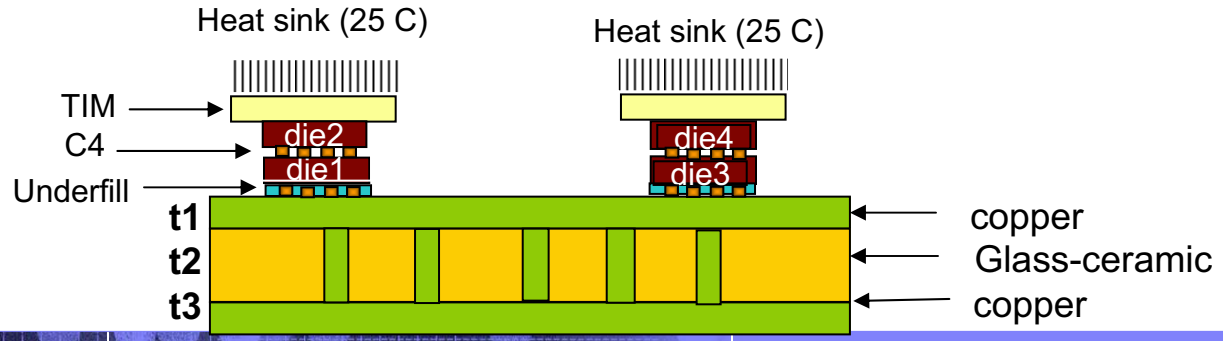

Geometry Parameters:

a= 20 cm, b= 20 cm
t1 = 36 micron
t2 = 350 micron
t3 = 36 micron
t_tim = 200 micron
t_die = 500 micron
t_underfil = 200 micron

Electrical Resistivity:

$$\rho_{C4\_Sn-0.7Cu} = 15e-8\ \Omega\cdot m$$

$$\rho_{Cu} = 1.8e-8\ \Omega\cdot m$$

$$\rho_{Tungsten} = 5.6e-8\ \Omega\cdot m$$

Thermal conductivities:

K_tim = 2 W/m-K
K_die = 110 W/m-K
K_underfil = 4.3 W/m-K.
K_glass-ceramic = 5 W/m-K
K_C4 = 40 W/m-K

TEMPERATURE DISTRIBUTION IN THE 1ST ITERATION BY GIT FOR IBM-GIT PROJECT

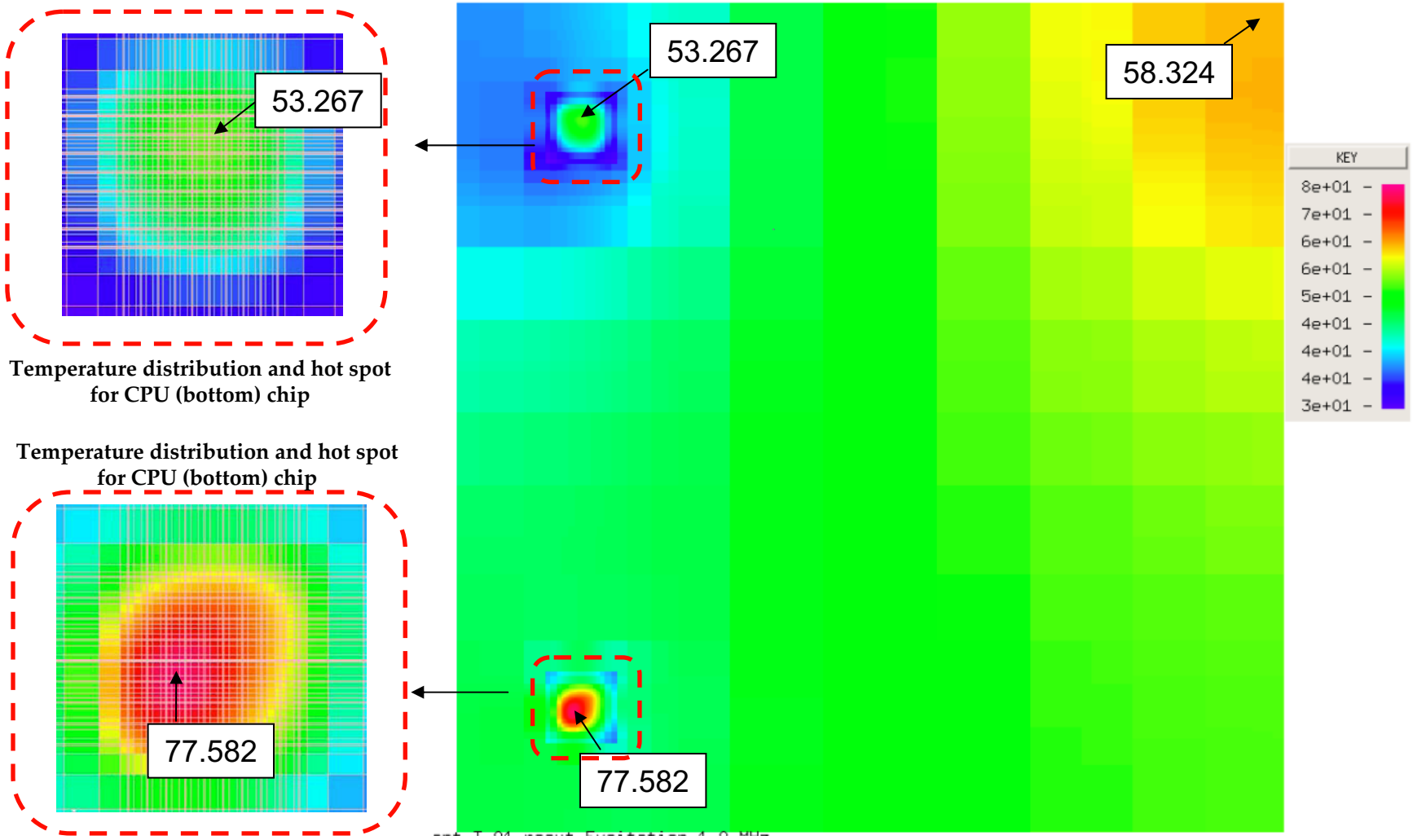

Temperature distribution and hot spot for CPU (bottom) chip

Temperature distribution and hot spot for CPU (bottom) chip

- The temperature distributions of substrate and bottom chips (cpu) are shown
- The hot spots are at not at the center of chips (different from uniform chip power map)

EQUIVALENT RESISTANCE NETWORK (NON UNIFORM POWER CHIPS) BY GIT

FOR IBM-GIT PROJECT

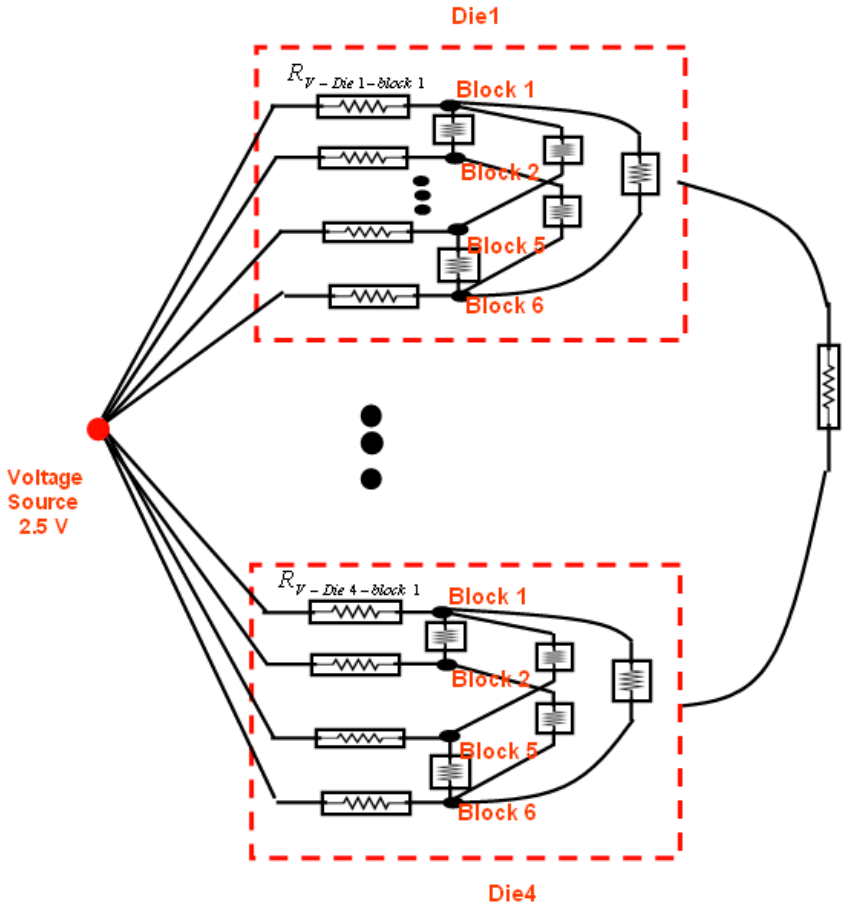

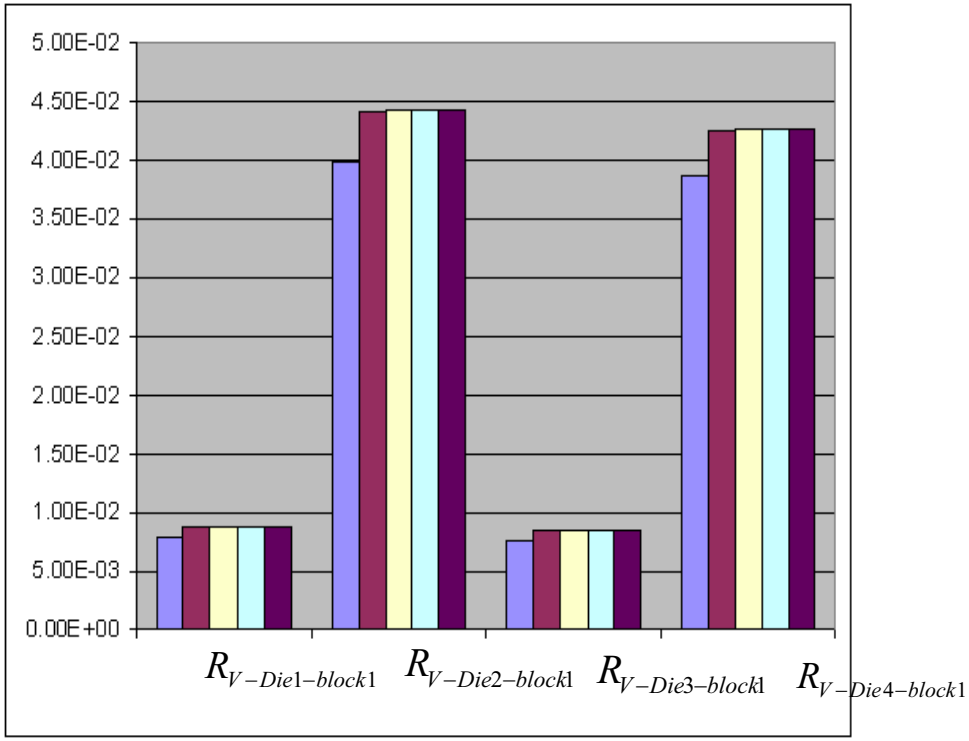

- Equivalent resistance also shows convergence.
- Compared to original value at room temperature, it grows about 10% because of Joule heating effect for both case.

CONCLUSIONS

- An automatic, multi-physics, general purpose framework was developed
- Electrical simulation scheme was used for thermal analysis without solver rewrite
- Extremely large problem sizes can be handled due to the computation power of the electrical algorithm
  - **Full BEOL stacks with full detail of all metals and dielectrics**
  - **Large multi-chip stacks**
  - **Complete accuracy is maintained in-spite of high density requirements**
- Various thermal boundary conditions, such as constant temperature, heat density, and joule heating can be created through this analogy.
- General 3D stacking, on-chip interconnect, and packaging structures could be analyzed through this scheme
- Electrical-thermal coupling simulation using a common solver has been developed

THANK YOU

Acknowledgement:

Collaborators from GIT, HKU, IBM, UIUC, AND UCSB